16th World Conference on Earthquake, 16WCEE 2017

Santiago Chile, January 9th to 13th 2017

Paper N° 4666

Registration Code: S-V1464724670

Model-based MDOF real-time hybrid simulation procedure considering time-delay effects

N. Li[(1)], Bille F. Spencer Jr[(2)], Zhong-Xian Li[(3)]

[(1)] *Associate Professor, School of Civil Engineering, Tianjin University / Key Laboratory of Coast Civil Structure Safety, Ministry of Education, Tianjin, China. neallee@tju.edu.cn.*

[(2)] *Professor, Department of Civil and Environmental Engineering, University of Illinois at Urbana-Champaign, Urbana, U.S.A. bfs@illinois.edu.*

[(3)] *Professor, School of Civil Engineering, Tianjin University / Key Laboratory of Coast Civil Structure Safety, Ministry of Education, Tianjin, China. zxli@tju.edu.cn.*

Abstract

A model-based real-time hybrid simulation (RTHS) method with a robust control algorithm which compensates the time-delay effect for the multi-actuator systems (1/5 scaled loading boundary condition box at UIUC with 6 degrees-of-freedom) is developed in this study. Unlike the conventional testing method, in RTHS the desired responses of the critical element, which are loaded using servo-hydraulic actuator system with a large or full scale model in a laboratory, are obtained by the experimental part. The behaviors of other elements under external excites are calculated by solving the dynamic equations of motion using a numerical model in the computational part. The control scheme proposed herein needs to directly address the servo-hydraulic and actuator dynamics through model-based robust control algorithm and considers the time-delay effect. The transfer functions are identified through the MIMO calibration procedure with the local linearization of the coordinate transformation between actuator coordinate system and Cartesian coordinate system. Based on the uncertainty characteristic, the robust controller for LBCB is implemented and compiled into the NI/LabView CompactRIO system. Furthermore, IIR filter is adopted and mitigated into the RTHS process based on NI/Labview platform for time-delay compensation in the control loop. The finite element simulation of a one-bay frame structure with a scaled column testing during RTHS is simulated on 2 NI cRIO system. At the same time, the sources of the time-delay effect in the dynamics of the RTHS system and the noise in the DSP system are directly incorporated. The proposed test procedure needs to be verified and validated by additional tests. Some conclusions can be drawn from the model-based RTHS test procedure. It is indicated that the model-based robust control design method is suitable for different complicated actuation models. The proposed test scheme allows for the testing of a broader class of structures in the RTHS.

Keywords: sub-structure method; time-delay; real-time hybrid simulation; Multi-input multi-output; robust control; nonlinear seismic response.

1. Introduction

The bearing capacity and the nonlinear performance of civil engineering structures subjecting the severe loads, such as earthquakes, winds, and tsunami, have been widely investigated in the past decades. To enhance researchers in understanding and analyzing an engineering structures precisely, experiment tests are widely carried out on both examining the structure/member's responses and validating the theory in analysis. Recently, the advanced hardware and software of experimental technique improves the structural design and analysis method distinctly. On the other hand, the requirement of complicated structural experimental test has stimulated and contributed to various test methods, such as shake table testing and pseudo-dynamic testing, mutually.

Recently, the sub-structural and distributed real-time hybrid simulation (RTHS)[1; 2] method, which is developed based on the pseudo-dynamic testing method[3], has been adopted to test the nonlinear performance of structures. In RTHS, the testing system is decomposed into experimental (physical) parts and computational parts (sub-structure components). The desired responses of the critical element, which are loaded using servo-hydraulic actuator systems at a large or full scale model in a laboratory, are obtained by the experimental parts. And the behaviors of other elements under external excitation are calculated by solving the dynamic equations of motion using a numerical model and integration algorithm in the computational parts. Nowadays, RTHS provides a solution to balance between the testing requirement of large scale structures and the size limitation of laboratories facility. And after years of development[4-10], it has become more feasible to make utility instead of shaking-table testing and pseudo dynamic testing.

Unlike the conventional testing method, there is an inevitable time-delay phenomenon in the RTHS testing. The causes of time-delay are separated into several reasons[11]: (1) time taken in the DAQ system for the sensor to process the data; (2) time taken in the calculation of the numerical sub-structure part and the transmission of the control signal to the actuator; (3) time taken by the actuator responding to actually displacement or force command. These time-delays affect the efficiency and robustness of the entire system, often leading to inaccurate results and driving the structure testing in to an unstable phenomenon[12].

Although the hardware of the experimental facility have quickly been improved during recent years, various software techniques, such as compensation control algorithms[12] and numerical integration schemes[13], have been developed to reduce the disadvantage of the time-delay effect. The compensation methods are based on constant time delay assumption[14], adaptive control theory[15; 16], multi-variable control algorithm[7; 17] and formulated in cascaded compensators[18], normally. Experimental studies indicated that the time-delay error cannot be completely eliminated no matter how sophisticated a compensation technique is used. Although it is possible to achieve almost-zero phase delay with proper control algorithm design, there is little research focused on the time-delay compensation and stability analysis for the multi-degree of freedom systems [12; 19; 20].

Once the transmission system time-delay is compensated properly (assuming the loading boundary conditions for physical sub-structure actuates accurately without delay), the numerical sub-structure computational delay is another issue need to be tackled, especially for the distributed computational model system[21]. For the complicated structure requiring high-fidelity numerical models, the numerical integration scheme often takes more time, which also causes computational time-delay. Many integration schemes have been used in RTHS to reduce the computational delay. The explicit integration scheme with unconditional stability has drawn much attention recently [13; 22-24]. Many researchers have developed different algorithms for different software/hardware platforms. Bonnet *et al.* [25] tested nonlinear series damper system with Newmark explicit scheme. Schellenberg[13] studied direct integration schemes (Newmark , generalized-alpha method), Runge-Kutta integration schemes and operator-splitting methods, systematically. Chen[22] proposed C-R unconditional stable explicit integration method. Ou[24] proposed modified Runge-Kutta method for RTHS. Wang et al [26] verified the feasibility to use large-step integration scheme in RTHS. However, there is few research focusing on both physical and numerical time-delay at the same time. The uncertainty of time-delay will occur at different time slot, the system stability needs more revision, especially for MDOF system.

The main content in this article is to establish a feasible test framework using the loading-boundary-condition-box (LBCB) at University of Illinois at Urbana and Champaign for RTHS. The LBCB dynamic model is deduced using frequency domain identification of multi-input, multi-output (MIMO) algorithm[27]. The dynamic MIMO system of LBCB is controlled using Compact RIO system (National Instruments). The numerical part of model is built in NI real-time operation system with multi-dimensional Bouc-Wen model. While the FEM is implemented into the inner loop of the system, the communication between other FEM model and the experiment controller may be established through OpenFresco and/or UI-Simcor using network communication protocol. For LBCB actions on structures, the target control command for each actuator is calculated based on the coordinate transformation (inverse kinematic transformation, IKT and forward kinematic transformation, FKT) algorithm, which is implemented into controller CompactRIO system. The time delay of actuation system and DAQ system is calibrated and is compensated using H_∞ control algorithm. For numerical part integration time step coupled with actuator action time step, the predict-corrector algorithm is modified for 6 DOF system on the real time operation system. Finally, a scaled hybrid simulation is carried out to verify the proposed framework and the result are discussed.

2. Model for Loading Boundary Condition Box (LBCB)

LBCBs come in different shapes and sizes in Civil and Environmental Engineering, UIUC. The facility has 3 large scale LBCBs whose actuators have a stroke length of 10 or 20 inches (0.254 or 0.51 m) and can push around 270 kips (1200 kN). The facility has 4 1/5 scale actuators with stroke lengths of 2 or 4 inches (0.051 or 0.102 m) that can push 1 to 3 kips (4.45 to 13.3 kN). In this paper, we are doing the test on the 1/5 scaled LBCB.

Each LBCB provides 6 degree-of-freedom actions and consists of a reaction box, as shown in Fig 1. The motion center of the loading platen is used to center rotations and moments of the LBCB onto the specimen boundary. The default motion center for the LBCB is on the bottom of the platen at the center when all of the actuators are at mid-stroke (Fig. 2).

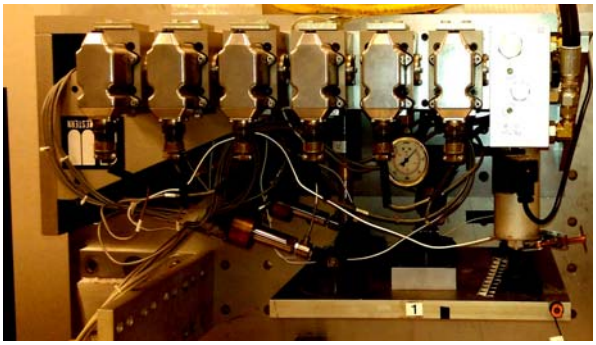

Fig 1. - Loading Boundary Condition-Box (LBCB, x-actuator on left)

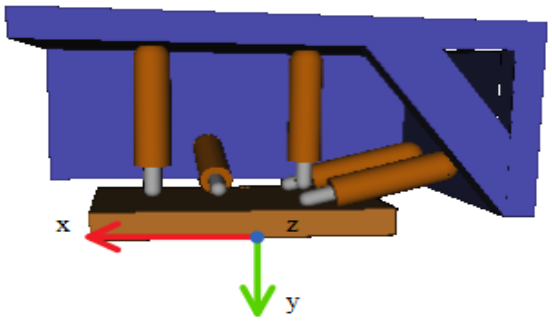

Fig 2. - Definition of LBCB loading motion center and coordinates (x-actuator on right)

2.1 Transformation from actuator to global coordinates

The control point of the LBCB is seldom at the bottom center of the platen when executing test. When doing RTHS, the action platen is driven by 6 actuators, and the control command from numerical model is on the Cartesian coordinate. The actuators and joint connections may not stay on the mid-stroke positions at all when carrying a test for different specimen setup. The motion of the platen must be calculated for different specimens.

Nakata *et al.* [28] proposed to use inverse kinematic transformation (IKT) and forward kinematic transformation (FKT) to deal with this problem. For small deformation test, the IKT approach was suitable and computed for convenience. OpenFresco[13] is not suitable for LBCB since there is no ExperiementalSetup class for LBCB implemented. In this study, a coupled 6 actuators setup is implemented into Labview real-time operation system.

As mentioned above, the piston action distance can be expressed as follow, which is also the coordinates' transformation matrix expression,

$$\Delta\mathbf{L} = \frac{\partial\mathbf{\Phi}}{\partial\mathbf{X}} \cdot \frac{\Delta\mathbf{X}}{2\mathbf{L}} \tag{1}$$

in which $\Delta\mathbf{L} = \{\Delta l_i\}^T$ is the increment in the actuator length, $\Delta\mathbf{X} = \{\Delta x\ \Delta y\ \Delta z\ \Delta\theta_x\ \Delta\theta_y\ \Delta\theta_z\}^T$ is the global displacement of the platen, and $\mathbf{\Phi}$ is a symbolic equation represents the transformation from global to actuator coordinates[28]. For 1/5 scaled LBCB (the *x*-axial actuators on the left side), when the specimen boundary loading center is at the center of the platen and the 6 actuators are at the mid-stroke position, the IKT and FKT matrices are given in Eq. (2) and Eq. (3).

$$\mathbf{\Phi}_{\text{IKT}} = \begin{bmatrix} 0.9518 & -0.0004 & 0.3068 & 1.4709 & -0.8015 & -4.5641 \\ 0.9518 & 0.0004 & 0.3068 & -1.4709 & -0.8015 & 4.5641 \\ -0.0159 & 0.9664 & 0.2566 & 4.7127 & 0.0896 & -0.0447 \\ -0.0002 & 0.004 & 1.0 & 0.0581 & 5.6258 & -0.0224 \\ 0.0023 & 0.0003 & 1.0 & 4.8102 & -6.011 & -0.0094 \\ 0.0023 & -0.0003 & 1.0 & -4.8102 & -6.011 & -0.0094 \end{bmatrix} \tag{2}$$

$$\mathbf{\Phi}_{\text{FKT}} = \begin{bmatrix} 0.5258 & 0.5254 & 0.0004 & -0.0943 & -0.1139 & -0.1145 \\ 0.0051 & 0.0125 & 1.0357 & -0.1468 & -0.5675 & 0.4432 \\ -0.0018 & 0.0007 & -0.0021 & 0.5170 & 0.2403 & 0.2437 \\ -0.0002 & 0.0002 & -0.0001 & 0.0000 & 0.1041 & -0.1040 \\ -0.0001 & 0.0003 & -0.0004 & 0.0860 & -0.0433 & -0.0427 \\ -0.1096 & 0.1096 & -0.0001 & 0.0 & 0.03359 & -0.0336 \end{bmatrix} \tag{3}$$

On the other hand, the response forces on each actuator need to be reversed into global coordinates. Those responses are used in the equilibrium equation iteration for the numerical structure model. Because the IKT is a nonlinear equation, a converged solution for IKT is obtained through the modified Newton-Raphson method.

2.2 Calibration of LBCB actuators

The model for the LBCB system is valuable for investigating the stability and robustness of the real-time hybrid testing technique. The frequency domain identification technique is adopted in this study. The MFDID[27] allowed accurate present the measured system transfer function for different test specimens. For different actuator, the hydraulic servo system is different.

The identified actuators frequency transformation functions are listed as below,

$$G_{x1} = \frac{1.0548\times10^9}{\left(s^2+88.2s+7842\right)\left(s^2+332.5s+1.438\times10^5\right)} \tag{4}$$

$$G_{x2} = \frac{6.8391\times10^8}{\left(s^2+79.35s+6140\right)\left(s^2+309.6s+1.223\times10^5\right)} \tag{5}$$

$$G_{y} = \frac{1.905\times10^9}{\left(s^2+105.5s+1.795\times10^4\right)\left(s^2+299.6s+1.119\times10^5\right)} \tag{6}$$

$$G_{z1} = \frac{1.4515\times10^{9}}{\left(s^2+88.19s+1.177\times10^{4}\right)\left(s^2+270.6s+1.308\times10^{5}\right)} \tag{7}$$

$$G_{z2} = \frac{2.5745\times10^{9}}{\left(s^2+94.48s+1.647\times10^{4}\right)\left(s^2+402.5s+1.648\times10^{5}\right)} \tag{8}$$

$$G_{z3} = \frac{2.5373\times10^{9}}{\left(s^2+95.9s+1.884\times10^{4}\right)\left(s^2+382.8s+1.424\times10^{5}\right)} \tag{9}$$

Taken into account of the uncertainties of actuators, the transfer function uncertainty region is shown in Fig. 3.

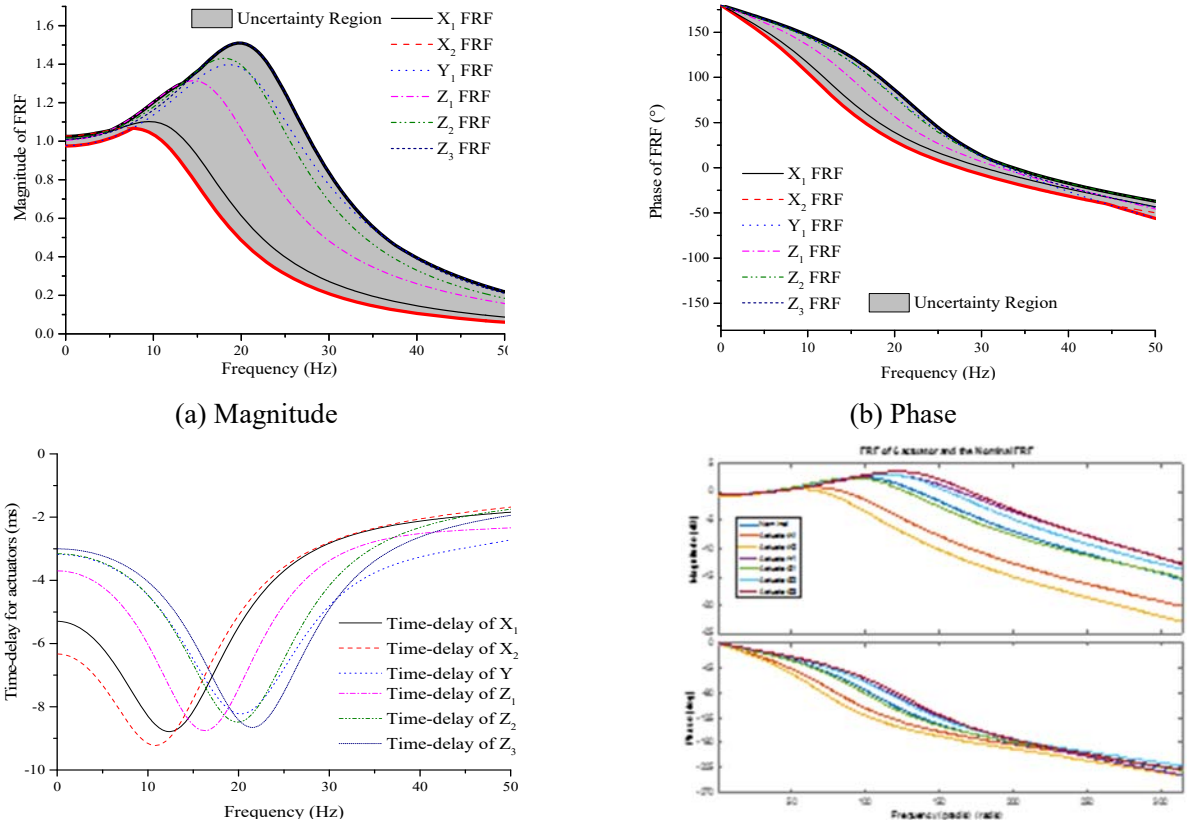

(a) Magnitude

(b) Phase

(c) Time-delay for different actuators

(d) Nominal system comparison

Fig. 3 – Frequency response plots for actuators (uncertainty and time-delay consideration)

2.3 Actuators coupled effects consideration

There is geometric interactive effect among the LBCB actuators. The system is clearly identified without structural specimen interaction and the coupled effect can be neglected in the model. As shown in Fig. 4., the totally 6 LBCB actuators' frequency response are identified at the same time.

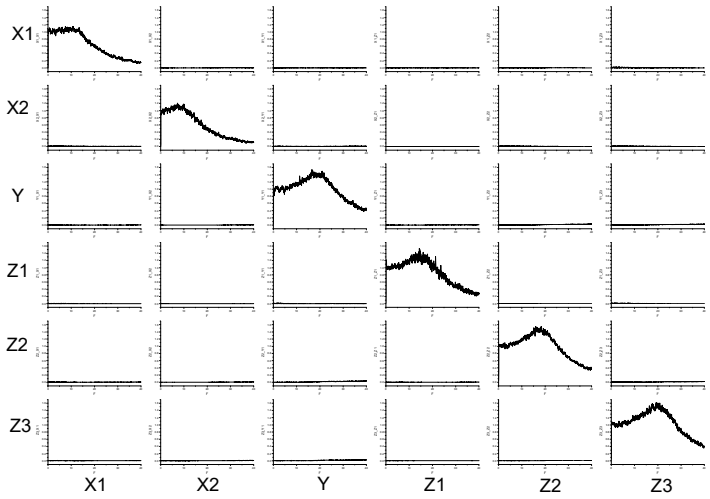

Fig. 4. – Cross and auto-relationship of frequency response functions for 6 actuators

However, the structure-control interaction (SCI) should be taken into account. The uncertainty model should be revised based on the stiffness contribution of the specimen to the dynamic system.

3. Model-based robust controller design for LBCB

3.1 General structure of robust control system

Typical robust controller design scheme with the system plant G, the controller K, the measured output y, the control signal u, the tracking error e, sensor noise n_s, and disturbance noise d, reference signal r are illustrated in Fig. 5. W_e, W_u and W_y is specified/designed filters for signal processing.

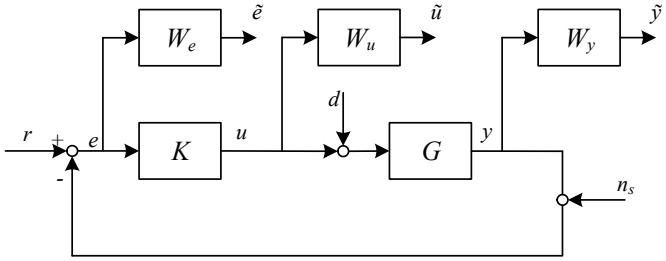

Fig. 5. – Standard control scheme for robust control

The sensitivity function is (from reference r to tracking error e or filtered error $\tilde{e}$)

$$T_{r\to e} = \left(I + GK\right)^{-1} \quad \text{or} \quad T_{r\to \tilde{e}} = W_e \left(I + GK\right)^{-1} \tag{10}$$

For the system perfromance or the signal tracking requirement, with low-pass filter W_e, the norm value $\left\|T_{r\to \tilde{e}}\right\|_\infty = \left\|W_e \left(I + GK\right)^{-1}\right\|_\infty$ must be small and the tracking error is small, such that y follows the reference input r well in the low frequency range. The robust or uncertainty stable requirement is represented through

$$T_{n_s\to \tilde{u}} = -W_u \left(I + GK\right)^{-1} K \tag{11}$$

and also the norm value with high pass filter W_y should be small for high frequency noise rejection,

$$T_{n_s \to \tilde{y}} = -W_y GK\left(I + GK\right)^{-1} \tag{12}$$

Combined one or several equation from (10)~(12), the general robust control problem and mixed optimal robust control problem can be formulated.

3.2 Model-based uncertainty model

In this paper, the nominal plant displacement transfer function for actuators, G_o,

$$G_{\mathrm{o}} = \frac{1.701\times10^{9}}{s^4 + 424.9s^3 + 1.799\times10^{5}s^2 + 1.698\times10^{7}s + 1.804\times10^{9}} \tag{13}$$

which is identified using MFDID[27]. By adopting the multiplicative uncertainty model, the actuator uncertainty model is

$$\Delta_m = \left(0.5642s^2 + 37.08s + 185.3\right)\Big/\left(s^2 + 78.39s + 5849\right) \tag{14}$$

The frequency response of nominal system is illustrated in Fig. 3(d). The loop-shaping H_∞ optimal design strategy is adopted for the model-based control algorithm.

3.3 Loop-Shaping design

The loop shaping method augments the plant with appropriately chosen weights so that the frequency response of the weighted plant is reshaped in order to meet the closed-loop performance requirements, then a robust controller is synthesized to meet the stability. This loop-shaping design can be carried out in the following 3 steps.

1. Using weighted compensator, W_1 and W_2, the nominal system G_o are modified or augmented to give a desired loop shape and form the shaped system, G, considering about the uncertainty. Then calculate the stability margin, $\varepsilon_{\max}$, as

$$\varepsilon_{\max} = \begin{cases} \left(\left\| \begin{bmatrix} K \\ I \end{bmatrix} \left(I - GK\right)^{-1} \begin{bmatrix} I & G \end{bmatrix} \right\|_\infty \right)^{-1} & K \text{ stabilises } G \\ 0 & \text{otherwise} \end{cases} \tag{15}$$

The margin also needs to satisfy

$$\varepsilon_{\max} = \sqrt{1 - \left\| \tilde{N} \quad \tilde{M} \right\|_\infty^2} < 1 \tag{16}$$

with $\tilde{M}$, $\tilde{N}$ the normalized coprime factors of G such that $G = \tilde{M}^{-1}\tilde{N}$.

2. Select a $\varepsilon \le \varepsilon_{\max}$ and synthesize a controller K_∞ that satisfies

$$\left\| \begin{bmatrix} K_\infty \\ I \end{bmatrix} \left(I - GK\right)^{-1} M^{-1} \right\|_\infty \le \frac{1}{\varepsilon_{\max}} \tag{17}$$

which is given by

$$K_\infty = \left[\begin{array}{c|c} A+BF+\gamma^2\left(L^T\right)^{-1}ZC^T\left(C+DF\right) & \gamma^2\left(L^T\right)^{-1}ZC^T \\ \hline B^TX & -D^T \end{array}\right] \tag{18}$$

with $F=-S^{-1}\left(D^TC+B^TX\right)$, $L=\left(1-\gamma^2\right)I+XZ$, $S=I+D^TD$, $R=I+DD^T$, and X and Z satisfied the two Ricatti equations given by

$$\begin{aligned} &\left(A-BS^{-1}D^TC\right)Z+Z\left(A-BS^{-1}D^TC\right)^T-ZC^TR^{-1}CZ+BS^{-1}B^T=0 \\ &\left(A-BS^{-1}D^TC\right)^TX+X\left(A-BS^{-1}D^TC\right)-XBS^{-1}B^TX+C^TR^{-1}C=0 \end{aligned} \tag{19}$$

3. The final feedback controller, K, is then constructed by combining the controller K_∞, with the weighting functions W_1 and W_2 such that $K=W_1K_\infty W_2$.

In this paper, the desired controller, G, is designed and expressed as

$$G=\frac{1.988\times10^5}{s^2+207.35s+3553.1} \tag{20}$$

The bode plots of designed system transfer function of nominal actuator system (G_o), sensitivity (S), complementary sensitivity function (T) and controller (K) are illustrated in Fig 6, respectively. The closed-loop system transfer function (CL) is mostly flatten in which the frequency region is interested.

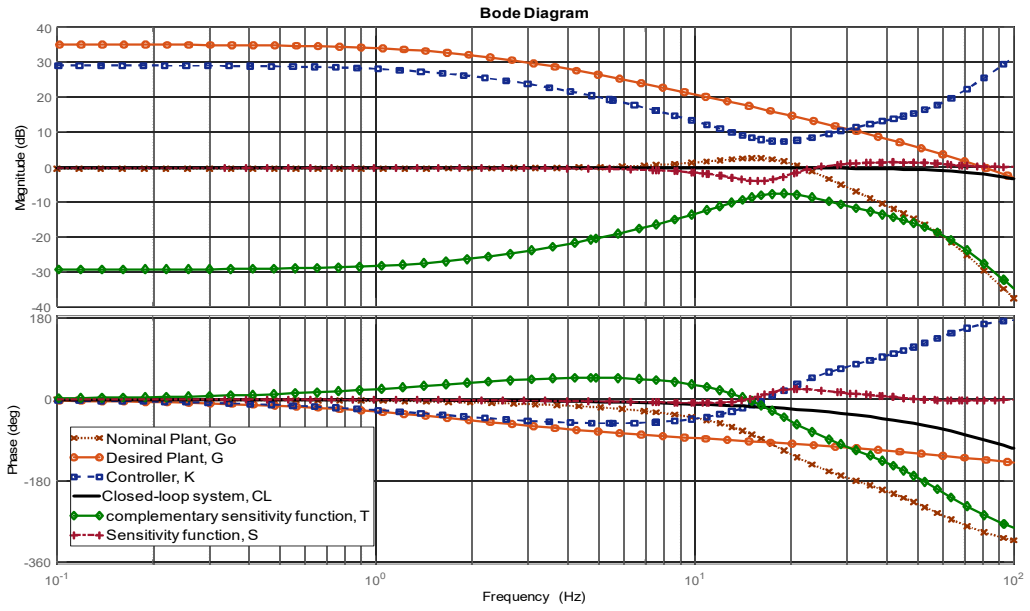

Fig. 6. – Singular value plot for sLBCB system and robust controller

The bode plot in Fig. 6 shows that the designed robust controller have a good performance in 0~50Hz, and the time-delay (the slope of phase) is no more than 2 samples (0~50Hz) for 2048Hz testing controller setting.

4 Real-time hybrid simulation setup

4.1 Structure model

Integrated software and hardware is necessary to be able to conduct RTHS in the laboratory[21]. In general, a fast computational solver needs to communicate with the controllers in the laboratory and bridges numerical and physical portions of the hybrid simulation testing system. In this implementation, the numerical model is compiled with Matlab/Simulink. The numerical model is a plane frame structure, which is illustrated in Figure 7.

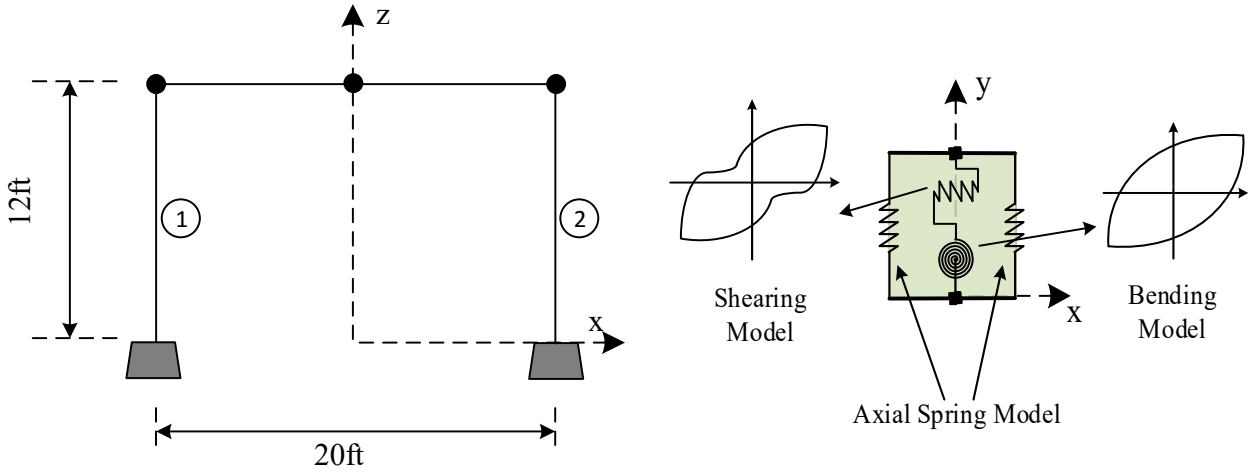

(a) structural model (b) column model

Fig. 7. – Simplified plane frame structure model

The column element 1 will tested physically, while the other part will be numerically simulated in Simulink and run on the cRIO[29] real-time operation system. When the experiment is carrying out, the real-time operation system is responsible for integrating the differential equation of dynamic system and calculating the deformation command for the testing specimen.

4.2 System design and time integration

In this research, the 1/5 scaled LBCB site test model is a scaled column member. The numerical part is implemented mostly upon different Bouc-Wen models, as in the Fig. 6(b). The idea is to present the nonlinear behavior of the column well and compute efficiently. For the actuator and the numerical column models, there are 3 DOFs each node. The conceptual loop for a single integration time step is demonstrated in Fig. 8.

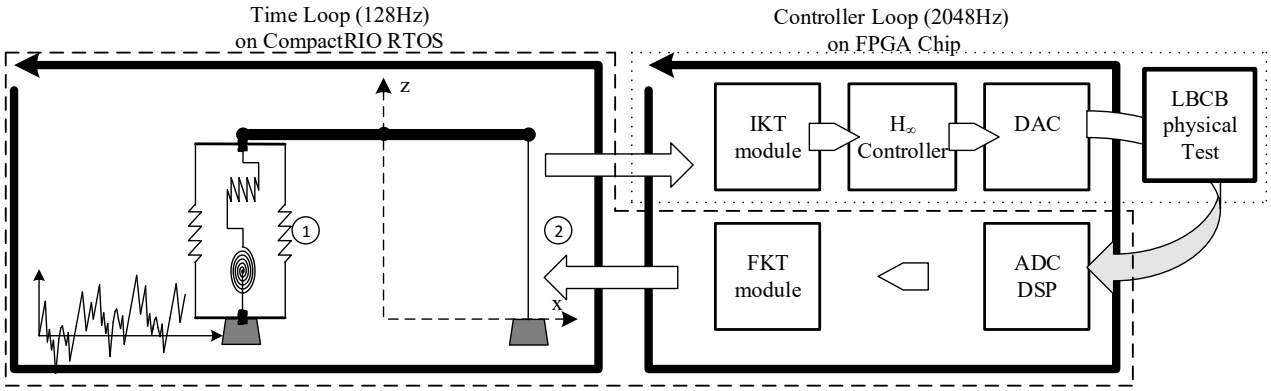

Fig. 8. – Proposed RTHS framework

In this study, the time-delay consumed by the numerical part in RTHS is eliminated by the simplified numerical modal which guarantees that the numerical integration can be finished within 1/128 sec. The numerical system and the robust controller (with DSP filter) are discretized with different loop frequencies for cRIO system and

FPGA system[29], respectively. For the numerical integration, the initial stiffness of the column is pre-configured for the RTHS in cRIO system.

4.3 Verification and compensation

A hybrid simulation is performed to examine the performance and the noise rejection efficiency using the identified plant model in Eq. (13) and the designed robust controller, K_∞. The left part of the system in the dash line sketched in Fig. 8 is implemented in a cRIO system using scan interface mode, it can access the FPGA module. The right part of the system in the dot line in Fig. 8 is implemented in a FPGA mode, which can access the analogy IO at a very high frequency. This part is also handling the physical test part. The two parts of the system are implemented on two cRIO hardware, separately. A group of 0~10Hz chirp signals at amplitude of 10 mm are used as the desired trajectory to drive the simulated LBCB system.

6. Conclusion

1). Model based robust control for the RTHS using LBCB facility.
In this study, the model based robust control algorithm for the actuator of LBCB is deduced based on transfer functions of the system and taken into account the uncertainty and time delay characteristic of different actuator. The parameters of the MIMO model were obtained using frequency domain identification techniques. The model for the LBCB system is valuable for investigating the stability and robustness of the real-time hybrid testing technique.
2). Time-delay effects.
Since the FEM analysis part of RTHS in this implementation is running on the real-time operation system with NI hardware, the effect of actuator time-delay is the most important one which was investigated for real-time hybrid simulation in this study. A comparison of the displacement responses showed good accuracy of the approach for the robust controller algorithms presented in this study. It should be noted that the nonlinear transformation matrix relating the Cartesian coordinate to the actuators coordinate has additional computational delay for LBCB controller. Time delay caused by the sensing and DAQ systems are relatively small for this system.
The model-based strategies and compensation techniques are appropriate solutions for the RTHS with time-delay effects. It is also worth noting that besides this specified facility, LBCB, the proposed RTHS scheme can also be applied to other commonly MIMO systems and hydraulic servo-actuator testing facilities. The time-delay effects can be compensated reasonable.

7. Acknowledgements

This work is sponsored by the National Basic Research Program (973 Program) of China under Grant No. 2011CB013603 and the Natural Science Foundations (51378341) and Tianjin Municipal Natural Science Foundation (Grant No. 13JCQNJC07200). This support is gratefully acknowledged.

8. References

[1] C. R. Thewalt, S. A. Mahin. Hybrid Solution Techniques for Generalized Pseudodynamic Testing [R]. EERC-87/09, Earthquake Engineering Research Center, College of Engineering, University of California, 1987.
[2] M. Nakashima, K. Ishii, S. Kamagata, H. Tsutsumi, K. Ando. Feasibility of Pseudo Dynamic Test Using Substructuring Techniques [C]. Proceedings of the Ninth World Conference on Earthquake Engineering. Tokyo, Japan, 1988.
[3] S. Mahin, P. Shing. Pseudodynamic Method for Seismic Testing [J]. *Journal of Structural Engineering*. 1985, **111**(7):1482-1503
[4] R. Christenson, Y. Lin, A. Emmons, B. Bass. Large-Scale Experimental Verification of Semiactive Control through Real-Time Hybrid Simulation [J]. *Journal of Structural Engineering*. 2008, **134**(4):522-534
[5] C. Chen, J. M. Ricles, T. L. Karavasilis, Y. Chae, R. Sause. Evaluation of a Real-Time Hybrid Simulation System for Performance Evaluation of Structures with Rate Dependent Devices Subjected to Seismic Loading [J]. *Engineering Structures*. 2012, **35**(Feb 2012):71-82

[6] K. M. Mosalam, S. Günay. Seismic Performance Evaluation of High Voltage Disconnect Switches Using Real-Time Hybrid Simulation: I. System Development and Validation [J]. *Earthquake Engineering & Structural Dynamics*. 2014, **43**(8):1205-1222

[7] S. Günay, K. M. Mosalam. Enhancement of Real-Time Hybrid Simulation on a Shaking Table Configuration with Implementation of an Advanced Control Method [J]. *Earthquake Engineering & Structural Dynamics*. 2015, **44**(5):657-675

[8] H. Xu, C. Zhang, H. Li, J. Ou. Real-Time Hybrid Simulation Approach for Performance Validation of Structural Active Control Systems: A Linear Motor Actuator Based Active Mass Driver Case Study [J]. *Structural Control and Health Monitoring*. 2014, **21**(4):574-589

[9] A. Friedman, S. Dyke, B. Phillips, R. Ahn, B. Dong, Y. Chae, N. Castaneda, Z. Jiang, J. Zhang, Y. Cha, A. Ozdagli, B. Spencer, J. C. Ricles, R., A. Agrawal, R. Sause. Large-Scale Real-Time Hybrid Simulation for Evaluation of Advanced Damping System Performance [J]. *Journal of Structural Engineering*. 2015, **141**(6):04014150

[10] T. Asai, C. Chang, B. Spencer, Jr. Real-Time Hybrid Simulation of a Smart Base-Isolated Building [J]. *Journal of Engineering Mechanics*. 2015, **141**(3):04014128

[11] A. K. Agrawal, Y. Fujino, B. K. Bhartia. Instability Due to Time Delay and Its Compensation in Active Control of Structures [J]. *Earthquake Engineering & Structural Dynamics*. 1993, **22**(3):211-224

[12] C. Chen, F. Sanchez, M. Khan. Effect of Actuator Delay on Real-Time Hybrid Simulation Involving Multiple Experimental Substructures [M]. Dynamics of Coupled Structures, Volume 4. Springer International Publishing, 2015pp. 9-17

[13] A. H. Schellenberg. Advanced Implementation of Hybrid Simulation [D]. University of California, Berkeley, 2008.

[14] T. Horiuchi, T. Konno. A New Method for Compensating Actuator Delay in Real–Time Hybrid Experiments [J]. *Philosophical Transactions of the Royal Society of London A: Mathematical, Physical and Engineering Sciences*. 2001, **359**(1786):1893-1909

[15] C. Chen, J. Ricles. Tracking Error-Based Servohydraulic Actuator Adaptive Compensation for Real-Time Hybrid Simulation [J]. *Journal of Structural Engineering*. 2010, **136**(4):432-440

[16] B. Phillips, B. Spencer, Jr. Model-Based Multiactuator Control for Real-Time Hybrid Simulation [J]. *Journal of Engineering Mechanics*. 2013, **139**(2):219-228

[17] B. M. Phillips, N. E. Wierschem, B. F. Spencer. Model-Based Multi-Metric Control of Uniaxial Shake Tables [J]. *Earthquake Engineering & Structural Dynamics*. 2014, **43**(5):681-699

[18] P.-C. Chen, K.-C. Tsai. Dual Compensation Strategy for Real-Time Hybrid Testing [J]. *Earthquake Engineering & Structural Dynamics*. 2013, **42**(1):1-23

[19] M. Nakashima, N. Masaoka. Real-Time on-Line Test for Mdof Systems [J]. *Earthquake Engineering & Structural Dynamics*. 1999, **28**(4):393-420

[20] C.-M. Chang, T. M. Frankie, B. F. Spencer, D. A. Kuchma. Multiple Degrees of Freedom Positioning Correction for Hybrid Simulation [J]. *Journal of Earthquake Engineering*. 2015, **19**(2):277-296

[21] G. Mosqueda, B. Stojadinovic, S. Mahin. Implementation and Accuracy of Continuous Hybrid Simulation with Geographically Distributed Substructures [R]. EERC 2005-02, 2005.

[22] C. Chen, J. M. Ricles, T. M. Marullo, O. Mercan. Real-Time Hybrid Testing Using the Unconditionally Stable Explicit Cr Integration Algorithm [J]. *Earthquake Engineering & Structural Dynamics*. 2009, **38**(1):23-44

[23] B. Wu, G. Xu, Q. Wang, M. S. Williams. Operator-Splitting Method for Real-Time Substructure Testing [J]. *Earthquake Engineering & Structural Dynamics*. 2006, **35**(3):293-314

[24] G. Ou, A. Prakash, S. Dyke. Modified Runge-Kutta Integration Algorithm for Improved Stability and Accuracy in Real Time Hybrid Simulation [J]. *Journal of Earthquake Engineering*. 2015, **19**(7):1112-1139

[25] P. A. Bonnet, C. N. Lim, M. S. Williams, A. Blakeborough, S. A. Neild, D. P. Stoten, C. A. Taylor. Real-Time Hybrid Experiments with Newmark Integration, Mcsmd Outer-Loop Control and Multi-Tasking Strategies [J]. *Earthquake Engineering & Structural Dynamics*. 2007, **36**(1):119-141

[26] F. Zhu, J.-T. Wang, F. Jin, Y. Gui, M.-X. Zhou. Analysis of Delay Compensation in Real-Time Dynamic Hybrid Testing with Large Integration Time-Step [J]. *Smart Structures and Systems, An Int'l Journal*. 2014, **14**(6):1269-1289

[27] S. Kim, B. Spencer, C. Yun. Frequency Domain Identification of Multi-Input, Multi-Output Systems Considering Physical Relationships between Measured Variables [J]. *Journal of Engineering Mechanics*. 2005, **131**(5):461-472

[28] N. Nakata, B. F. Spencer Jr, A. S. Elnashai. Multi-Dimensional Mixed-Mode Hybrid Simulation Control and Applications [R]. 1940-9826, Newmark Structural Engineering Laboratory. University of Illinois at Urbana-Champaign., 2007.

[29] National Instruments. NI Labview for Compactrio Developer's Guide [EB/OL]. https://www.ni.com/compactriodevguide/. 2016.